Hindawi Publishing Corporation
Advances in OptoElectronics
Volume 2014, Article ID 397681, 9 pages
http://dx.doi.org/10.1155/2014/397681

Research Article

The CdS/CdSe/ZnS Photoanode Cosensitized Solar Cells Basedon Pt, CuS, Cu_2S, and PbS Counter Electrodes

Tung Ha Thanh,[1] Dat Huynh Thanh,[2] and Vinh Quang Lam[3]

[1] *Faculty of Physics, Dong Thap University, Dong Thap Province, Cao Lanh City 870000, Vietnam*
[2] *Vietnam National University, Ho Chi Minh City 700000, Vietnam*
[3] *University of Science, Vietnam National University, Ho Chi Minh City 700000, Vietnam*

Correspondence should be addressed to Tung Ha Thanh; tunghtvlcrdt@gmail.com

Received 14 October 2013; Revised 25 December 2013; Accepted 25 December 2013; Published 27 February 2014

Academic Editor: Armin Gerhard Aberle

Highly ordered mesoporous TiO_2 modified by CdS, CdSe, and ZnS quantum dots (QDs) was fabricated by successive ionic layer adsorption and reaction (SILAR) method. The quantity of material deposition seems to be affected not only by the employed deposition method but also and mainly by the nature of the underlying layer. The CdS, CdSe, and ZnS QDs modification expands the photoresponse range of mesoporous TiO_2 from ultraviolet region to visible range, as confirmed by UV-Vis spectrum. Optimized anode electrodes led to solar cells producing high current densities. Pt, CuS, PbS, and Cu_2S have been used as electrocatalysts on counter electrodes. The maximum solar conversion efficiency reached in this work was 1.52% and was obtained by using Pt electrocatalyst. CuS, PbS, and Cu_2S gave high currents and this was in line with the low charge transfer resistances recorded in their case.

1. Introduction

As an alternative to dye molecules, semiconductor quantum dots (QDs) like CdS, CdSe [1], PbS [2], InAs [3], InP [4], and others [5] as well as extremely thin inorganic absorber layers [6, 7] have been used. QDs are very attractive because of their size-dependent optical band gap, the possibility to design hierarchical multilayer absorber structures, and the potential to use them for multiexciton generation from a single photon. One potential method for improving the performance of quantum dots solar cells (QDSSCs) is by constructing desired energy band structures using multiple QDs. Niitsoo and coworkers have firstly demonstrated that a desired cascade structure can be formed by sequential deposition of CdS and CdSe layers onto the TiO_2 nanoparticle films [8]. Recently, Lee et al. have also reported a self-assembled TiO_2/CdS/CdSe structure that exhibited a significant enhancement in the photocurrent response [9, 10]. In addition, nanostructured CuS, PbS, Cu_2S, and Pt have been used as electrocatalysts on the counter electrode. Alternative catalysts have been proposed by several researchers [9–12]. Metal sulfides are considered a good choice. However, their deposition on plain FTO electrodes does not always produce materials with sufficiently high specific surface or with structural stability.

In this paper, we studied the effects of comodification by CdS, CdSe, and ZnS QDs on the photovoltaic response of mesoporous TiO_2 based QDSSC. The mesoporous TiO_2 were treated by SILAR of CdS, CdSe, and ZnS QDs and were used as photoanodes in QDSSC. We demonstrated that the comodified mesoporous TiO_2 possesses superior photovoltaic response compared to the single QD sensitized devices. Pt, CuS, PbS, and Cu_2S have been used as electrocatalysts on counter electrodes. The final TiO_2/CdS/CdSe/ZnS photoanode leads to high efficiency QDSSCs.

2. Experiment

2.1. Materials. $Cd(CH_3COO)_2{\cdot}2H_2O$ (99%), $Cu(NO_3)_2$, Na_2S, $Zn(NO_3)_2$, Se powder, S powder, Na_2SO_3, and Brass foil were obtained from Merck. TiO_2 paste was obtained from Dyesol, Australia.

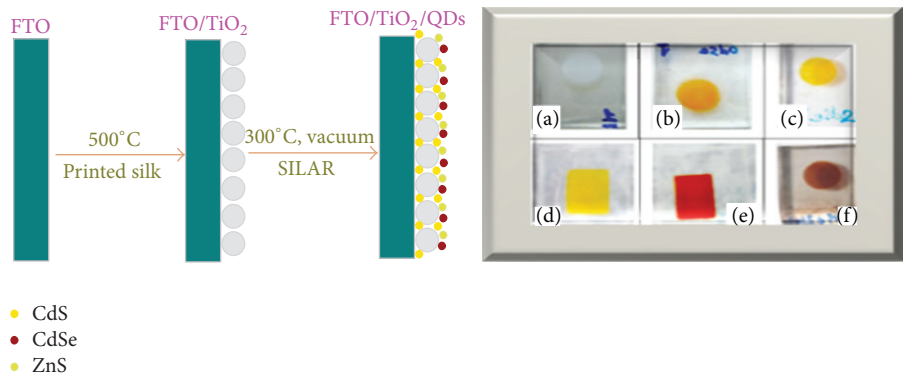

Figure 1: The diagram shows the process to prepare the TiO_2/CdS/CdSe/ZnS photoanode.

2.2. To Prepare TiO_2 Films. The TiO_2 thin films were fabricated by silk-screen printing with commercial TiO_2 paste. Their sizes ranged from 10 to 20 nm. Two layers of film with thickness of 8 μm were measured by microscope. Then, the TiO_2 film was heated at 400°C for 5 min and 500°C for 30 min. Afterwards, the film was dipped in 40 mmol $TiCl_4$ solution for 30 min at 70°C and heated at 500°C for 30 min.

The specific surface area of the mesoporous TiO_2 was investigated by using the N_2 adsorption and desorption isotherms before and after the calcination. The surface area is 120.6 $m^2\,g^{-1}$ (measured by BET devices). This result indicates that the synthesized material has wider mesoporous structure.

2.3. To Prepare TiO_2/CdS/CdSe/ZnS Films. The highly ordered TiO_2 was sequentially sensitized with CdS, CdSe, and ZnS QDs by SILAR method. First, the TiO_2 film was dipped in 0.5 mol/L $Cd(CH_3COO)_2$-ethanol solution for 5 min, rinsed with ethanol, dipped for 5 min in 0.5 mol/L Na_2S-methanol solution, and then rinsed with methanol. The two-step dipping procedure corresponded to one SILAR cycle and the incorporated amount of CdS QDs was increased by repeating the assembly cycles for a total of three cycles. For the subsequent SILAR process of CdSe QDs, aqueous Se solution was prepared by mixing Se powder and Na_2SO_3 in 50 mL pure water after adding 1 mol/L NaOH at 70°C for 7 h. The TiO_2/CdS samples were dipped into 0.5 mol/L $Cd(CH_3COO)_2$-ethanol solution for 5 min at room temperature, rinsed with ethanol, dipped in aqueous Se solution for 5 min at 50°C, and rinsed with pure water. The two-step dipping procedure corresponds to one SILAR cycle. Repeating the SILAR cycle increases the amount of CdSe QDs (a total of four cycles). The SILAR method was also used to deposit the ZnS passivation layer. The TiO_2/CdS/CdSe samples were coated with ZnS by alternately dipping the samples in 0.1 mol/L $Zn(NO_3)_2$ and 0.1 mol/L Na_2S-solutions for 5 min/dip, rinsing with pure water between dips (a total of two cycles). Finally, it was heated in a vacuum environment with different temperatures to avoid oxidation (see Figure 1). The thickness of TiO_2/CdS/CdSe/ZnS photoanodes were measured by Microscopic. The results of the average thickness of every layer of CdS, CdSe, and ZnS are 40 nm, 43.3 nm, 40 nm, respectively.

2.4. Construction of the Counter Electrodes. PbS films were deposited on fluorine doped tin oxide (FTO) conductive glass electrode by cyclic voltammetry (CV) from the solution of $Pb(NO_3)_2$ 1.5 mM and $Na_2S_2O_3$ 1.5 mM. CV experiments were carried out at various potential scan rates in a potential range 0.0 to –1.0 V versus Ag/AgCl/KCl electrode, pH from 2.4 to 2.7, and ambient temperature. Pt films were fabricated by silk-screen printing with commercial Pt paste. Then, the Pt films were heated at 450°C for 30 min. CuS was also deposited on FTO electrodes by a SILAR procedure, by modifying the method presented in [13]. Precursor solutions contained 0.5 mol/L $Cu(NO_3)_2$ in methanol and 1 mol/dm^3 $Na_2S{\cdot}9H_2O$ in a 1 : 1 water : methanol mixture. An FTO electrode was immersed for 5 min in the metal salt solution, copiously washed with triple-distilled water, dried in an air stream, immersed for 5 min in the $Na_2S{\cdot}9H_2O$ solution, and finally washed and dried again. This sequence again corresponds to one SILAR cycle. 10 SILAR cycles were performed. Finally, the electrode with deposited CuS film was first dried and then it was put for 5 min in an oven at 100°C. The counter electrode was a Cu_2S film fabricated on brass foil. Brass foil was immersed into 37% HCl at 70°C for 5 min, rinsed with water, and dried in air. After that, the etched brass foil was dipped into 1 mol/L S and 1 mol/L Na_2S aqueous solution, resulting in a black Cu_2S layer forming on the foil [14].

2.5. Fabrication of QDSSCs. The polysulfide electrolyte used in this work was prepared freshly by dissolving 0.5 M Na_2S, 0.2 M S, and 0.2 M KCl in Milli-Q ultrapure water/methanol (7 : 3 by volume). The CdS/CdSe/ZnS cosensitized TiO_2 photoanode and Pt counter electrode were assembled into a sandwich cell by heating with a Surlyn. The electrolyte was filled from a hole made on the counter electrode, which was later sealed by thermal adhesive film and a cover glass. The active area of QDSSC was 0.38 cm^2.

2.6. Characterizations and Measurements. The morphology of the prepared samples was observed using field-emission scanning electron microscopy (FE-SEM, S4800). The crystal

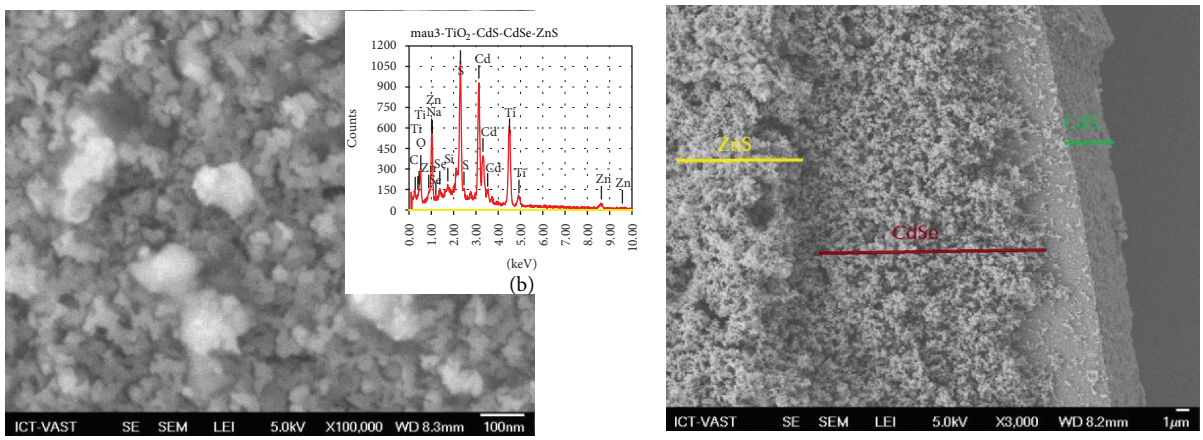

Figure 2: (a) FE-SEM images of the TiO_2/CdS/CdSe/ZnS photoanode, (b) energy dispersive analysis of X-ray spectra (EDAX) of the TiO_2/CdS/CdSe/ZnS photoanode, (c) cross-sectional view of the TiO_2/CdS/CdSe/ZnS photoanode.

structure was analyzed with an X-ray diffractometer (Philips, PANalytical X'pert, CuKα radiation). The absorption properties of the nanotube array samples were investigated using a diffuse reflectance UV-Vis spectrometer (JASCO V-670). Photocurrent voltage measurements were performed on a Keithley 2400 sourceMeter using a simulated AM 1.5 sunlight with an output power of 100 mW/cm^2 produced by a solar simulator (Solarena, Sweden).

3. Results and Discussion

Shown in Figures 2(a) and 2(b) are the FESEM images of TiO_2/CdS/CdSe/ZnS photoanode film. Figure 2(a) shows highly uniform porous morphology with the average inner diameter of nanostructure around 60 nm. For photovoltaic applications, the structure of QDs adsorbed TiO_2 should meet at less two criteria. First, the QDs should be uniformly deposited onto the TiO_2 surface without aggregation, so that the area of TiO_2/QDs can be maximized. Second, a moderate amount the QDs should be deposited so that TiO_2 is not blocked.

Figure 2(c) is a cross-sectional image showing that the QDs are well deposited onto the TiO_2 with an average thickness of about 12 μm by the microscope. Figure 2(b) is the energy dispersive X ray spectroscopy of the TiO_2/CdS/CdSe/ZnS film. It shows that the Ti and O peaks are from the TiO_2 film; and Cd, Se, Zn, and S peaks, clearly visible in the EDS spectrum, are from the QDs. The Si is from the FTO and C is from the solvent organic. That shows that the QDs are well deposited onto the TiO_2.

The structure of the TiO_2/QDs photoelectrodes for photovoltaic applications, shown in Figure 3(a), is studied by the XRD patterns. It reveals that the TiO_2 has an anatase structure with a strong (101) peak located at 25.4°, which indicates that the TiO_2 films are well crystallized and grow along the (101) direction (JCPDS Card number 21-1272). Three peaks can be observed at 26.4°, 44°, and 51.6°, which can be indexed to (111), (220), and (331) of cubic CdS (JCPDS Card number 41-1049) and CdSe (JCPDS Card number 75-5681), respectively. Two peaks can be observed at 48° and 54.6°, which can be indexed to (220) and (331) of cubic ZnS, respectively. It demonstrates that the QDs have been crystallized onto the TiO_2 film. Figure 3(b) is the Raman spectrum of the TiO_2/QDs photoelectrodes. It shows that an anatase structure of the TiO_2 films has five oscillation modes corresponding wave numbers at 143, 201, 395, 515, and 636 cm^{-1}. In addition, two peaks can be observed at 201, 395, and 515 cm^{-1}, which can be indexed to the cubic structure of CdS and CdSe. The results of the Raman are likely similar to the results of the XRD. The optical performance of the QDs coated TiO_2 film is characterized by absorbance. Figure 3(c) shows the UV-Vis absorption spectra of the sensitized electrodes measured after each cycle of SILAR. As expected, the absorbance increased with the deposition cycles of CdS, CdSe, and ZnS. However, only absorption spectra with SILAR cycles of the electrode TiO_2/CdS(3)/CdSe(3)/ZnS(2) show the best photovoltaic performance as discussed in the following section. In short-wavelength region (380–550 nm), the increase of absorbance is due to the fact that more CdS was loaded on TiO_2 film and the coabsorption of CdS, CdSe, and ZnS. In long-wavelength region (550–629 nm), the deposition of higher amounts of CdSe and ZnS on TiO_2/CdS electrode results in the increase of absorbance. Moreover, the increasing successive deposition cycles also trigger a red shift of absorption spectrum which is due to a slight loss of quantum confinement effect [15]. The evaluated sizes of CdS and CdSe are consistent with the sizes measured from the FE-SEM images. The effect of deposition cycles of CdS, CdSe, and ZnS can be clearly seen on the energy band gap values of CdS/CdSe/ZnS cosensitized TiO_2 films. The estimated band gaps vary from 1.97 eV to 2.7 eV, which are higher than the values reported for CdS and CdSe in bulk (2.25 eV and 1.7 eV resp.[16]), indicating that the sizes of CdS, CdSe, and ZnS on TiO_2 films are still within the scale of QDs. The diameter of QDs was calculated from 2 nm to 6 nm by (1). A higher absorption is thus obtained because

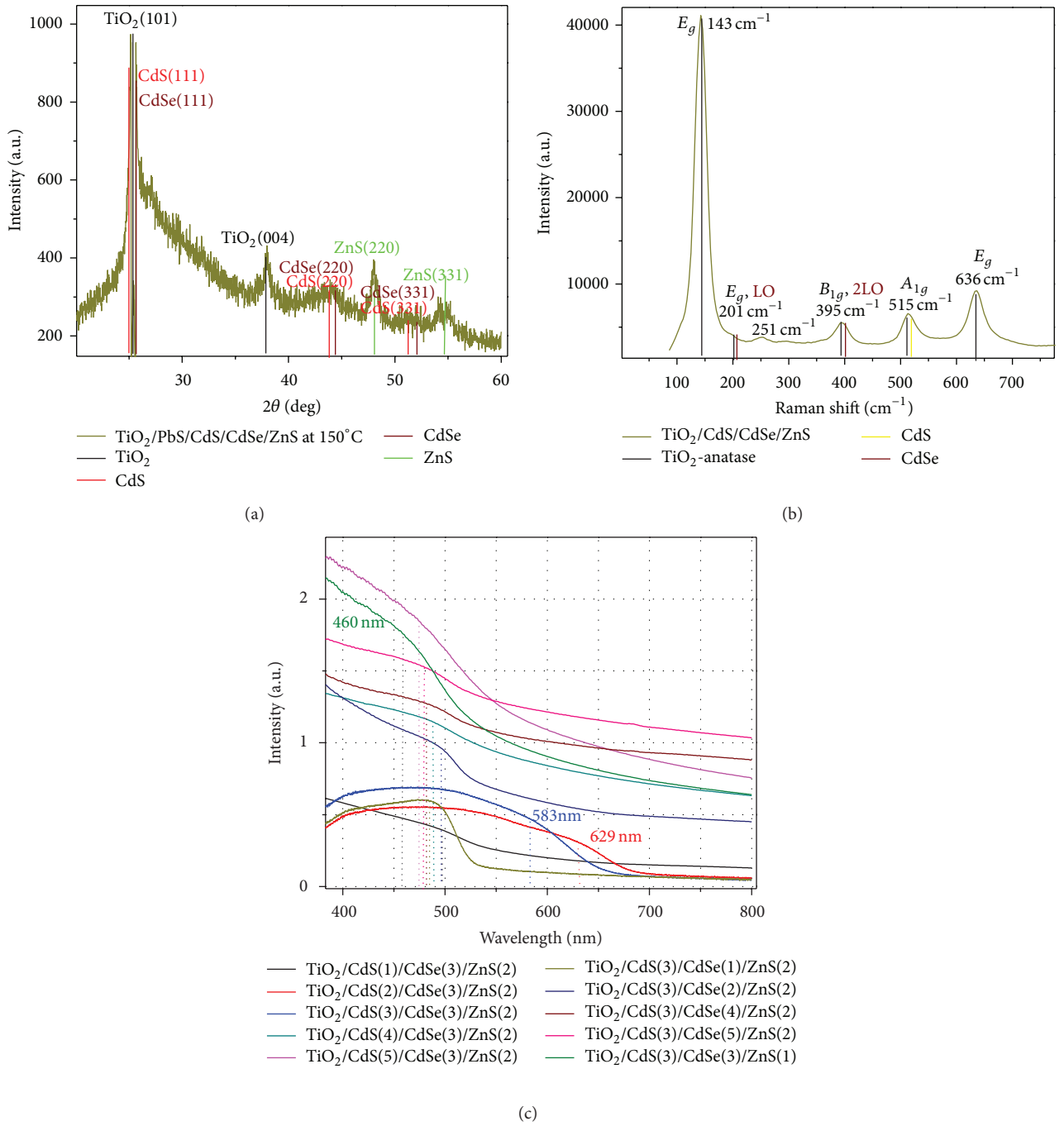

Figure 3: XRD (a), Raman (b), and UV-Vis (c) of the TiO_2/CdS/CdSe/ZnS photoanodes.

the absorption spectrum of ZnS complements those of the CdSe and CdS QDs. Furthermore, ZnS acts as a passivation layer to protect the CdS and CdSe QDs from photocorrosion [17]. Consider the following equation by Yu et al. [18] group:

$$D = 1.6122 \cdot 10^{-9}\lambda^4 - 2.6575 \cdot 10^{-6}\lambda^3 + 1.6242 \cdot 10^{-3}\lambda^2 - 0.4277\lambda + 41.57. \quad (1)$$

The XRD patterns were used to characterize the crystal structure of the obtained products. As shown in Figure 4(a), it can be seen that the XRD pattern of the PbS counter electrode is in conformity with cubic ($a = b = c = 5.93$ Å). The observed peaks could be assigned to diffraction from the (111), (200), (220), (311), and (222) faces and there is no characteristic peak for other impurities. This indicates that pure crystalline PbS was formed via the cyclic voltammetry process. Figure 4(b) illustrates the XRD pattern of the synthesized Cu_2S after

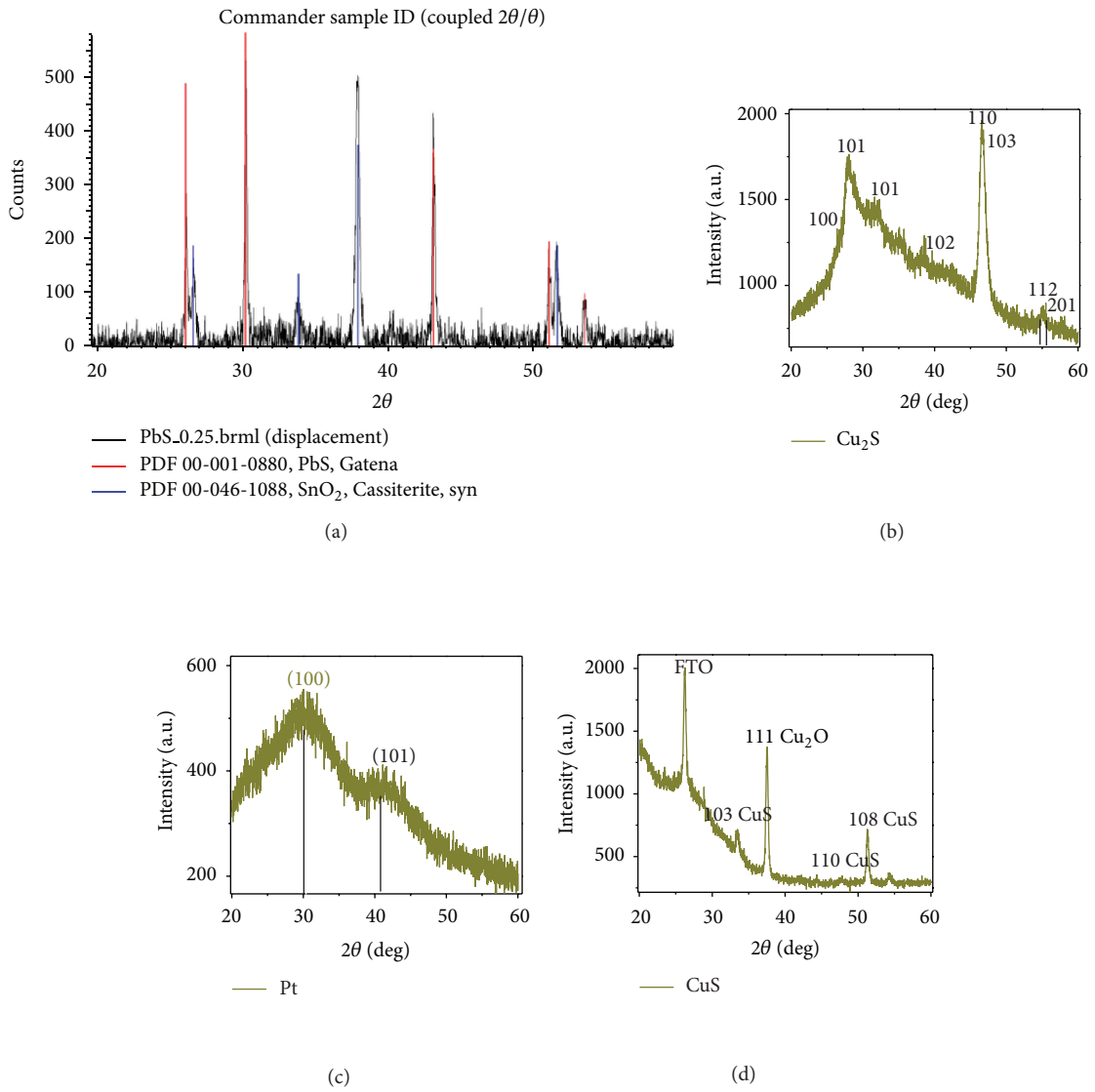

Figure 4: XRD of the PbS, Cu_2S, Pt, and CuS counter electrodes.

1 h by chemical bath deposition (CBD) method. The peaks of corresponding crystal planes were indexed in the figure, matching to the hexagonal phase chalcocite β-Cu_2S (JCPDS card number 46-1195, $a = 3.96$ Å, $c = 6.78$ Å). Figure 4(c) illustrates that the XRD pattern of the Pt films were fabricated by silk-screen printing with commercial Pt paste. The peaks of corresponding crystal planes were indexed in the figure, matching to the hexagonal phase. As shown in Figure 4(d), it can be seen that the XRD pattern of the CuS counter electrode is in conformity with the hexagonal phase. It is in agreement with the reported data for CuS (JCPDS Card. number 79-2321).

A relative energy level of different components is shown in Figure 5(a). According to the data reported in the literature [16, 19], the band gap of TiO_2 (3.2 eV) limits its absorption range below the wavelength of about 400 nm. CdSe has a higher conduction band (CB) edge than TiO_2, which is favorable for electron injection. However, with a band gap of 1.7 eV, the absorption of bulk CdSe is also limited below approximately 760 nm. The conduction band of CdSe is slightly lower than that of TiO_2, so the electrons would flow from CdSe to TiO_2 [20]. In addition, we have coated two layers of ZnS QDs, which could be attributed to several reasons. First, as the absorption edge of ZnS is at about 345 nm, a higher absorption can be obtained due to the complement of the absorption spectrum of the ZnS with that of the CdSe and CdS QDs. Second, ZnS acts as a passivation layer to protect the CdS and CdSe QDs from photocorrosion. Thus, the photoexcited electrons can efficiently transfer into the conduction band of TiO_2. Third, the outer ZnS layer can also be considered to be a potential barrier between the interface of QDs materials and the electrolyte. ZnS has a very wide band gap of 3.6 eV; it is much wider than that on the CdS and CdSe QDs. As a result, the leakage of electrons from the ZnS, CdSe, and CdS QDs into the electrolyte can be inhibited. As a result, an ideal model for the cosensitized

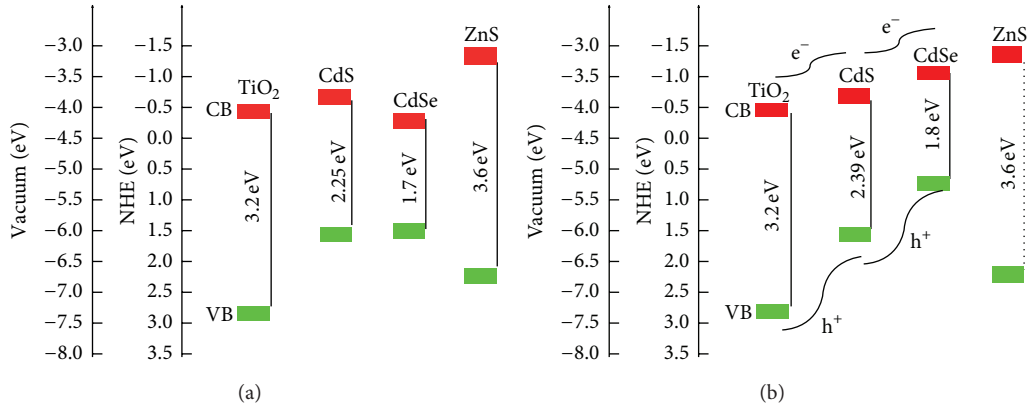

FIGURE 5: (a) Relative energy levels of TiO_2, CdS, CdSe, and ZnS in bulk phase, (b) the proposed energy band structure of the TiO_2/CdS/CdSe/ZnS nanostructure interface. All the energy levels are referenced to NHE scale. CB and VB are conduction band and valence band [16, 19].

TiO_2 electrode is shown in Figure 5(b). After CdSe and ZnS QDs are sequentially deposited onto a TiO_2/CdS film, A cascade type energy band structure is constructed for the cosensitized photoanode. The best electron transport path is from the conduction band of ZnS and finally reaching the conduction band of TiO_2. Meanwhile, this stepwise structure is also favorable for the hole transport.

We prepared the photoanodes with many different layers of QDs. Firstly, we have prepared CdS or CdSe films. However, the results were of very low performance. Therefore, we decided covering with ZnS layer for the following reasons. Firstly, extend peak adsorption spectrum in the visible light region. Secondly, the ZnS layers which acted as the agent passivated the surface of QDs. Moreover, they protected the light corrosion. Thus, the conversion excited electrons through the conduction band of TiO_2 better. Thirdly, ZnS layers separated the surfaces of the CdS and CdSe with electrolyte. The ZnS has a very wide band gap of about 3.6 eV, much larger than other CdS and CdSe QDs. As a result, electrons move from CdS, CdSe, and ZnS to the electrolyte can be inhibited. Figure 6(a) shows that the power conversion efficiencies of QDSSCs are increasing with the SILAR cycle number of CdS, CdSe, and ZnS at 3, 3, and 2, respectively. It is noted that lower power conversion efficiency was obtained for those cells with either less than 3 CdS and CdSe SILAR cycles or more than 3 CdS and CdSe SILAR cycles (Figure 6(b)). The TiO_2/CdS(3)/CdSe(3)/ZnS device shows an open-circuit voltage (V_{OC}) of 0.76 V, a short-circuit current density (J_{sc}) of 4.79 mA/cm^2, fill factor (FF) of 0.41, and an energy conversion efficiency of 1.52%. When the deposition cycles of CdS and CdSe increase, slight changes in V_{OC} and FF values were obtained. Remarkably, the J_{sc} decreases, which results in a substantial reduction of efficiency from 1.52% to 0.45% (Table 1). These results indicate that although better light absorption performance was obtained when more CdSe was loaded on TiO_2/CdS, the excessive CdSe on TiO_2/CdS films may lead to an increase of recombination in photoanodes. On the contrary, the increase of ZnS leads to the increasing generation of photoelectron and is helpful to collect excited electrons from ZnS, CdSe, and CdS to TiO_2 film.

FF is determined from measurement of the IV curve and is defined as FF $= V_{max} \cdot I_{Max}/V_{OC} \cdot I_{sc}$. FF depending on V_{OC} values, the junction quality (related with the series R_s), and the type of recombination in a solar cell. From Table 1, V_{OC} values change according to the film thickness from 0.29 to 0.76, corresponding to the change in FF from 0.26 to 0.41. Therefore, the FF is the low value because V_{OC} is low. On the other hand, V_{OC} values depend on the recombination process; they are particularly large; V_{OC} gives low open-circuit voltages. In addition, FF is effected by R_s. The equations of R_s can be calculated by Thongpron and coworkers [21] as follows:

$$R_s = \frac{V_1 - V_2}{I_2 - I_1} - \frac{1}{\lambda (I_2 - I_1)} \ln \left[\frac{I_{ph} + I_o - I_1}{I_{ph} + I_o - I_2} \right]. \quad (2)$$

Two operating points are (I_1, V_1) and (I_2, V_2) on a single I-V curve. $\lambda = q/nKT$; I_{ph}, I_o are the photocurrent and the diode reverse saturation current. R_s values are calculated from 55 to 158 mΩcm^{2-}. This result indicate that fill factor will decrease when VOC increase.

Four main types of counter electrodes have been studied. Their synthesis is detailed in experiment and method. The FESEM images of the corresponding electrocatalytic films are shown in Figure 7 (*inset*). In the first case, PbS films were deposited on fluorine doped tin oxide (FTO) conductive glass electrode by cyclic voltammetry (CV) from the solution of $Pb(NO_3)_2$ 1.5 mM and $Na_2S_2O_3$ 1.5 mM. CV experiments were carried out at various potential scan rates in a potential range 0.0 to −1.0 V versus Ag/AgCl/KCl electrode, pH from 2.40 to 2.70, and ambient temperature. CuS was also deposited on FTO electrodes by a SILAR procedure, by modifying the method presented in [13]. The electrode with deposited CuS film was first dried and then it was put for 5 min in an oven at 100°C. The counter electrode was a Cu_2S film fabricated on brass foil. Brass foil was immersed into 37% HCl at 70°C for 5 min and then rinsed with water and

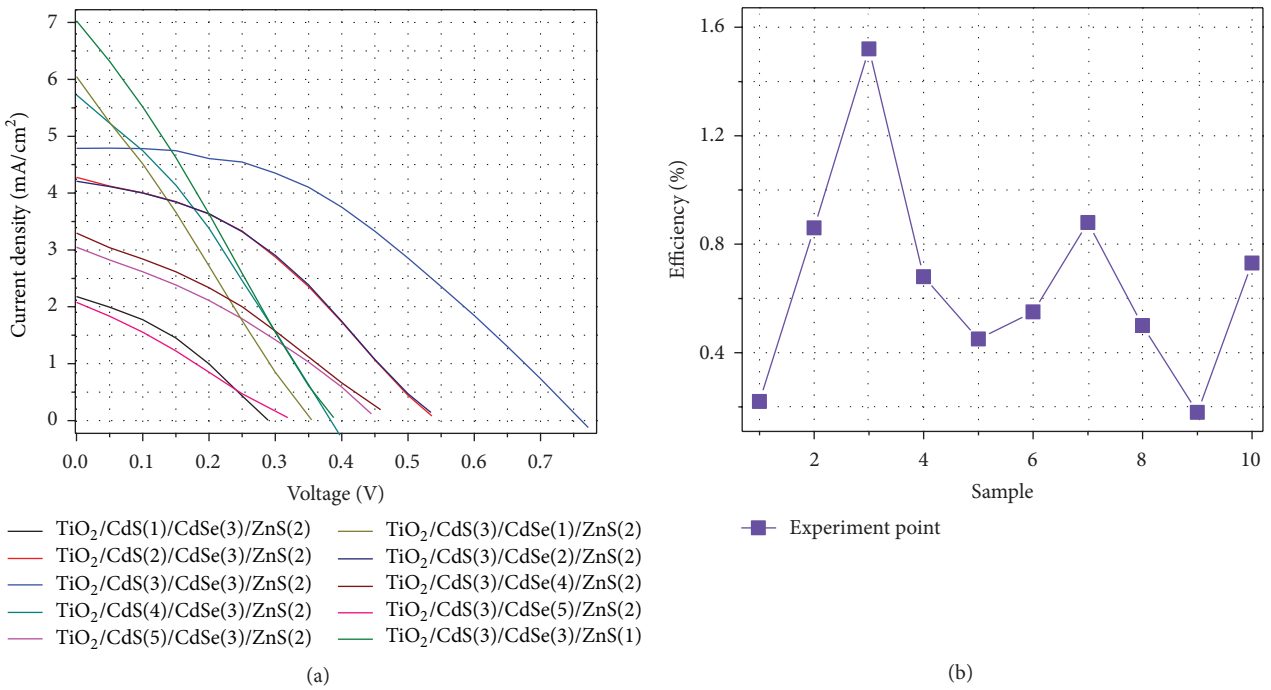

Figure 6: (a) The J-V curves of the QDSSCs with different photoanodes under one sun illumination and (b) diagram shows the values efficiency of solar cells.

Table 1: Photovoltaic performance parameters of QDSSCs based on different photoanodes.

Solar cells	J_{sc} (mA/cm^2)	V_{OC} (V)	Fill factor FF	Efficiency η (%)
TiO$_2$/CdS(1)/CdSe(3)/ZnS(2)	2.18	0.29	0.35	0.22
TiO$_2$/CdS(2)/CdSe(3)/ZnS(2)	4.28	0.54	0.37	0.86
TiO$_2$/CdS(3)/CdSe(3)/ZnS(2)	4.79	0.76	0.41	1.52
TiO$_2$/CdS(4)/CdSe(3)/ZnS(2)	5.73	0.39	0.31	0.68
TiO$_2$/CdS(5)/CdSe(3)/ZnS(2)	3.05	0.45	0.32	0.45
TiO$_2$/CdS(3)/CdSe(1)/ZnS(2)	6.05	0.356	0.256	0.55
TiO$_2$/CdS(3)/CdSe(2)/ZnS(2)	4.21	0.55	0.38	0.88
TiO$_2$/CdS(3)/CdSe(4)/ZnS(2)	3.30	0.48	0.31	0.50
TiO$_2$/CdS(3)/CdSe(5)/ZnS(2)	2.08	0.33	0.27	0.18
TiO$_2$/CdS(3)/CdSe(3)/ZnS(1)	7.03	0.39	0.26	0.73

Table 2: Photovoltaic parameters of solar cell modified by various cathodes.

Solar cells	J_{sc} (mA/cm^2)	V_{OC} (V)	Fill factor FF	Efficiency η (%)
PbS cathode	6.14	0.43	0.24	0.63
CuS cathode	5.72	0.38	0.31	0.68
Cu$_2$S cathode	4.2	0.55	0.376	0.87
Pt cathode	4.79	0.76	0.41	1.52

dried in air. After that, the etched brass foil was dipped into 1 mol/L S and 1 mol/L Na_2S aqueous solution, resulting in a black Cu_2S layer forming on the foil [14]. Figures 4(a), 4(b), and 4(c) show the image of PbS, CuS, Cu_2S films that present a rough nanostructure, which are suitable for counter electrodes. The similar Pt films were fabricated by silk-screen printing with commercial Pt paste. Then, the Pt films were heated at 450°C for 30 min. In the high magnification image of Figure 4(d), one can distinguish the big blocks of FTO covered with Pt nanoparticles [22]; Figure 4 and Table 2 show that the maximum efficiency reached in the present work, that is, 1.52%, was obtained with Pt on the counter

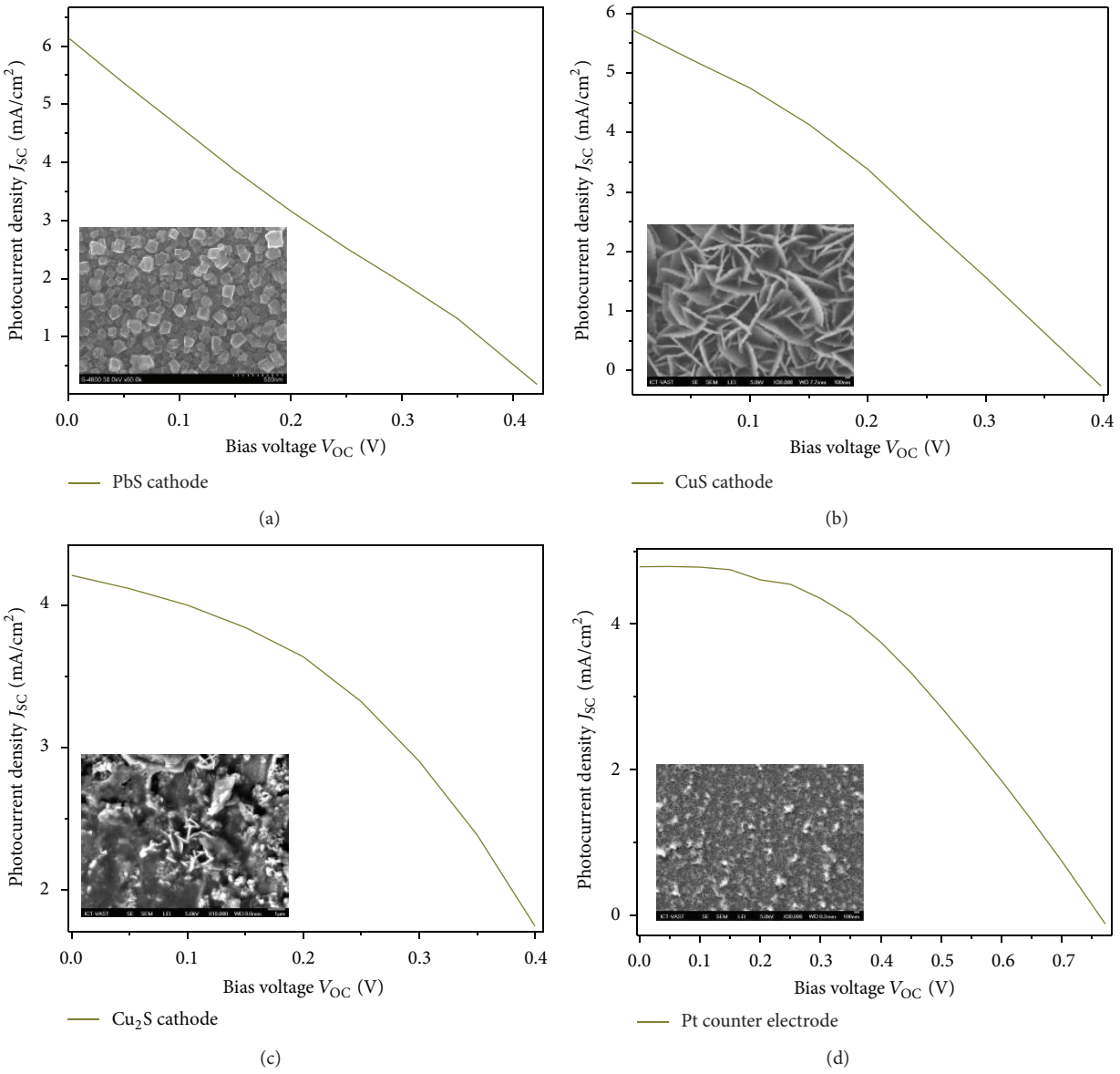

Figure 7: J-V curves of solar cells modified by various cathodes.

electrode. The Pt electrocatalysts, that is, Cu_2S, CuS, and PbS, gave higher current densities than Pt but lower V_{OC} than Pt. On the contrary, open-circuit voltage values were practically not affected by the electrocatalyst. The major problem encountered in the present work was with the value of the fill factor (FF). It remained below 0.42 and this limited the overall efficiency, even though, the current densities presently recorded were high. The search for a higher FF is an open question and has occupied many other researchers. It is believed that higher FFs will be obtained with even better electrocatalysts and more functional counter electrodes.

4. Conclusions

QDSSCs have been constructed and optimized by combining TiO_2 with CdS, CdSe, and ZnS nanostructure on the anode electrode. PbS, CuS, Cu_2S, and Pt were used as electrocatalysts on counter electrodes in combination with a polysulfide electrolyte. The maximum solar conversion efficiency of 1.52% was obtained with a Pt counter electrode. The most important finding of this work is the importance of the first nanostructure layer deposited on the mesoporous TiO_2 film, which affected the quantity and the quality of the subsequent QDs layers and the ensuing cell efficiency. High current densities were obtained with all cells having optimized anode electrodes. Among them, the highest currents were obtained with Pt electrocatalysts.

Conflict of Interests

The authors declare that there is no conflict of interests regarding the publication of this paper.

Acknowledgments

This work was supported by Vietnam National University with the name of the project being B 2012-18-05TD, the University of Science of Ho Chi Minh City, and Dong Thap University.

References

[1] M. Shalom, S. Ruhle, I. Hod et al., "Energy level alignment in CdS quantum dot sensitized solar cells using molecular dipoles," *Journal of the American Chemical Society*, vol. 131, no. 29, pp. 9876–9877, 2009.

[2] P. Yu, K. Zhu, A. G. Norman, S. Ferrere, A. J. Frank, and A. J. Nozik, "Nanocrystalline TiO_2 solar cells sensitized with InAs quantum dots," *Journal of Physical Chemistry B*, vol. 110, no. 50, pp. 25451–25454, 2006.

[3] A. Zaban, O. I. Mićić, B. A. Gregg, and A. J. Nozik, "Photosensitization of nanoporous TiO_2 electrodes with InP quantum dots," *Langmuir*, vol. 14, no. 12, pp. 3153–3156, 1998.

[4] S. Rühle, M. Shalom, and A. Zaban, "Quantum-dot-sensitized solar cells," *ChemPhysChem*, vol. 11, no. 11, pp. 2290–2304, 2010.

[5] C. Herzog, A. Belaidi, A. Ogacho, and T. Dittrich, "Inorganic solid state solar cell with ultra-thin nanocomposite absorber based on nanoporous TiO_2 and In_2S_3," *Energy and Environmental Science*, vol. 2, no. 9, pp. 962–964, 2009.

[6] S.-J. Moon, Y. Itzhaik, J.-H. Yum, S. M. Zakeeruddin, G. Hodes, and M. Grätzel, "Sb_2S_3-Based mesoscopic solar cell using an organic hole conductor," *Journal of Physical Chemistry Letters*, vol. 1, no. 10, pp. 1524–1527, 2010.

[7] M. Shalom, J. Albero, Z. Tachan, E. Martínez-Ferrero, A. Zaban, and E. Palomares, "Quantum dot-dye bilayer-sensitized solar cells: breaking the limits imposed by the low absorbance of dye monolayers," *Journal of Physical Chemistry Letters*, vol. 1, no. 7, pp. 1134–1138, 2010.

[8] O. Niitsoo, S. K. Sarkar, C. Pejoux, S. Rühle, D. Cahen, and G. Hodes, "Chemical bath deposited CdS/CdSe-sensitized porous TiO_2 solar cells," *Journal of Photochemistry and Photobiology A*, vol. 181, no. 2-3, pp. 306–313, 2006.

[9] Y. L. Lee and Y. S. Lo, "Highly efficient quantum-dot-sensitized solar cell based on co-sensitization of CdS/CdSe," *Advanced Functional Materials*, vol. 19, no. 4, pp. 604–609, 2009.

[10] Y. L. Lee, C. F. Chi, and S. Y. Liau, "CdS/CdSe co-sensitized TiO_2 photoelectrode for efficient hydrogen generation in a photoelectrochemical cell," *Chemistry of Materials*, vol. 22, no. 3, pp. 922–927, 2010.

[11] A. L. Efros, M. Rosen, M. Kuno, M. Nirmal, D. J. Norris, and M. Bawendi, "Band-edge exciton in quantum dots of semiconductors with a degenerate valence band: dark and bright exciton states," *Physical Review B*, vol. 54, no. 7, pp. 4843–4856, 1996.

[12] L. E. Brus, "Electron-electron and electron-hole interactions in small semiconductor crystallites: the size dependence of the lowest excited electronic state," *The Journal of Chemical Physics*, vol. 80, p. 4403, 1984.

[13] T.-L. Li, Y.-L. Lee, and H. Teng, "High-performance quantum dot-sensitized solar cells based on sensitization with $CuInS_2$ quantum dots/CdS heterostructure," *Energy and Environmental Science*, vol. 5, no. 1, pp. 5315–5324, 2012.

[14] J. Tian, R. Gao, Q. Zhang et al., "Enhanced performance of CdS/CdSe quantum dot cosensitized solar cells via homogeneous distribution of quantum dots in TiO_2 film," *The Journal of Physical Chemistry C*, vol. 116, no. 35, pp. 18655–18662, 2012.

[15] H. M. Pathan and C. D. Lokhande, "Deposition of metal chalcogenide thin films by successive ionic layer adsorption and reaction (SILAR) method," *Bulletin of Materials Science*, vol. 27, pp. 85–111, 2004.

[16] M. Grätzel, "Photoelectrochemical cells," *Nature*, vol. 414, no. 6861, pp. 338–344, 2001.

[17] Z. Tachan, M. Shalom, I. Hod, S. Rühle, S. Tirosh, and A. Zaban, "PbS as a highly catalytic counter electrode for polysulfide-based quantum dot solar cells," *Journal of Physical Chemistry C*, vol. 115, no. 13, pp. 6162–6166, 2011.

[18] W. W. Yu, L. Qu, W. Guo, and X. Peng, "Experimental determination of the extinction coeicient of CdTe, CdSe and CdS nanocrystals," *Chemistry of Materials*, vol. 15, no. 14, pp. 2854–2860, 2003.

[19] C. G. Van de Walle and J. Neugebauer, "Universal alignment of hydrogen levels in semiconductors, insulators and solutions," *Nature*, vol. 423, no. 6940, pp. 626–628, 2003.

[20] Y. L. Lee and Y. S. Lo, "Highly efficient quantum-dot-sensitized solar cell based on Co-sensitization of CdS/CdSe," *Advanced Functional Materials*, vol. 19, no. 4, pp. 604–609, 2009.

[21] J. Thongpron, K. Kirtikara, and C. Jivacate, "A method for the determination of dynamic resistance of photovoltaic modules under illumination," in *Proceedings of the Technical Digest of the 14th International Photovoltaic Science and Engineering Conference (PVSEC14 '04)*, Bangkok, Thailand, January 2004.

[22] N. Balis, T. Makris, V. Dracopoulos, T. Stergiopoulos, and P. Lianos, "Quasi-solid-state dye-sensitized solar cells made with poly(3,4-ethylenedioxythiophene)-functionalized counter-electrodes," *Journal of Power Sources*, vol. 203, pp. 302–307, 2012.